Development 139, 1874-1884 (2012) doi:10.1242/dev.047589

DE-Cadherin regulates unconventional Myosin ID and Myosin IC in *Drosophila* left-right asymmetry establishment

Astrid G. Petzoldt[1,2], Jean-Baptiste Coutelis[1,*], Charles Géminard[1,*], Pauline Spéder[1,3], Magali Suzanne[1,4], Delphine Cerezo[1] and Stéphane Noselli[1,‡]

SUMMARY

In bilateria, positioning and looping of visceral organs requires proper left-right (L/R) asymmetry establishment. Recent work in *Drosophila* has identified a novel situs inversus gene encoding the unconventional type ID myosin (MyoID). In *myoID* mutant flies, the L/R axis is inverted, causing reversed looping of organs, such as the gut, spermiduct and genitalia. We have previously shown that MyoID interacts physically with β-Catenin, suggesting a role of the adherens junction in *Drosophila* L/R asymmetry. Here, we show that DE-Cadherin co-immunoprecipitates with MyoID and is required for MyoID L/R activity. We further demonstrate that MyoIC, a closely related unconventional type I myosin, can antagonize MyoID L/R activity by preventing its binding to adherens junction components, both in vitro and in vivo. Interestingly, DE-Cadherin inhibits MyoIC, providing a protective mechanism to MyoID function. Conditional genetic experiments indicate that DE-Cadherin, MyoIC and MyoID show temporal synchronicity for their function in L/R asymmetry. These data suggest that following MyoID recruitment by β-Catenin at the adherens junction, DE-Cadherin has a twofold effect on *Drosophila* L/R asymmetry by promoting MyoID activity and repressing that of MyoIC. Interestingly, the product of the vertebrate situs inversus gene inversin also physically interacts with β-Catenin, suggesting that the adherens junction might serve as a conserved platform for determinants to establish L/R asymmetry both in vertebrates and invertebrates.

KEY WORDS: DE-Cadherin, Left-right asymmetry, Myo31DF, Myosin IC, Myosin ID, Shotgun, *Drosophila*, Myo61F

INTRODUCTION

L/R patterning is required for the functional organization of the body plan and the L/R asymmetric development of visceral organs, such as the heart, liver or intestine in human. To date, two distinct molecular mechanisms responsible for symmetry breaking have been identified in vertebrates (for a review, see Levin, 2006; Levin and Palmer, 2007; Speder et al., 2007). The earliest known event is the left-sided expression of ion pumps in the early *Xenopus* embryo generating an asymmetric gap junction-mediated ion flow, leading to a directional transport of putative L/R determinants through the induced polarized electric field (Levin et al., 2002). The second mechanism operates during gastrulation and relies on tilted motile cilia localized at the embryonic node, which create a leftward fluid flow over the midline of the body leading to unidirectional transport and polarized accumulation of L/R determinants (for a review, see Raya and Belmonte, 2006). Propagation and maintenance of the initial asymmetric L/R signal is ensured by the expression of an asymmetric gene cascade, including the left-sided expression of *Nodal* and its downstream target genes *Pitx2* and *Lefty* (for reviews, see Raya and Belmonte, 2006; Tabin, 2006).

Most of the defects associated with aberrant L/R patterning lead to a randomization of L/R asymmetric traits (situs ambiguus), causing severe congenital disorders and embryonic lethality (Aylsworth, 2001). By contrast, rare but highly instrumental situs inversus mutations lead to a complete inversion of the L/R axis. To date, only two situs inversus genes have been molecularly identified in animal models: the inversin (*Inv*; *Invs* – Mouse Genome Informatics) gene in mouse (Yokoyama et al., 1993) and, more recently, *myosin ID* (*myoID*; *Myo31DF* – FlyBase) in *Drosophila melanogaster* (Hozumi et al., 2006; Speder et al., 2006). MyoID has been shown to act as an L/R determinant responsible for the clockwise (dextral) rotation of genitalia in male flies as well as the stereotyped looping of tubular organs, such as the embryonic gut, spermiduct and testis (Fig. 1A) (Ádám et al., 2003; Coutelis et al., 2008; Hozumi et al., 2006; Speder et al., 2006; Speder and Noselli, 2007; Speder et al., 2007; Suzanne, 2010). Loss of MyoID function causes a situs inversus phenotype characterized by counter-clockwise (sinistral) genitalia rotation and inverted organ looping. MyoID is required functionally in a critical time-window of 3 hours (Fig. 1A), one day before genitalia rotation occurs (Speder et al., 2006). The *myoID* gene encodes an unconventional type ID myosin: a one-headed, monomeric actin-based motor, bearing an N-terminal motor head domain, a neck domain with two IQ motifs and a short basic tail domain (Mooseker and Cheney, 1995).

A first hint towards the cellular function of MyoID came from the discovery of a physical interaction between this protein and the adherens junction component β-Catenin (Speder et al., 2006). The MyoID tail domain binds to β-Catenin in vitro and both proteins colocalize in vivo at the adherens junctions in the A8 segment of the male genital disc, the L/R organizer for genitalia (Fig. 1A). Adherens junctions are adhesive cell-cell contacts and signalling platforms, localizing apically in epithelial cells (Miyoshi and Takai, 2008). Their core component is the dimeric Ca^{2+}-dependent transmembrane protein E-Cadherin, establishing cell adhesion through extracellular domain binding of homodimers at the apical surfaces of adjacent cells (Niessen and Gottardi, 2008).

[1]Institute of Biology Valrose, University of Nice Sophia-Antipolis, UMR7277-CNRS, UMR1091 INSERM, Parc Valrose, 06108 Nice Cedex 2, France. [2]Center for Biological Systems Analysis, University of Freiburg; Habsburger Str. 49, 78104 Freiburg, Germany. [3]The Gurdon Institute; University of Cambridge; Tennis Court Road, Cambridge CB2 1QN, United Kingdom. [4]Laboratory of Cellular and Molecular Biology of Cell Proliferation (LBCMCP) UMR5088, University Paul Sabatier, 31062 Toulouse, France.

*These authors contributed equally to this work
‡Author for correspondence (noselli@unice.fr)

Accepted 6 March 2012

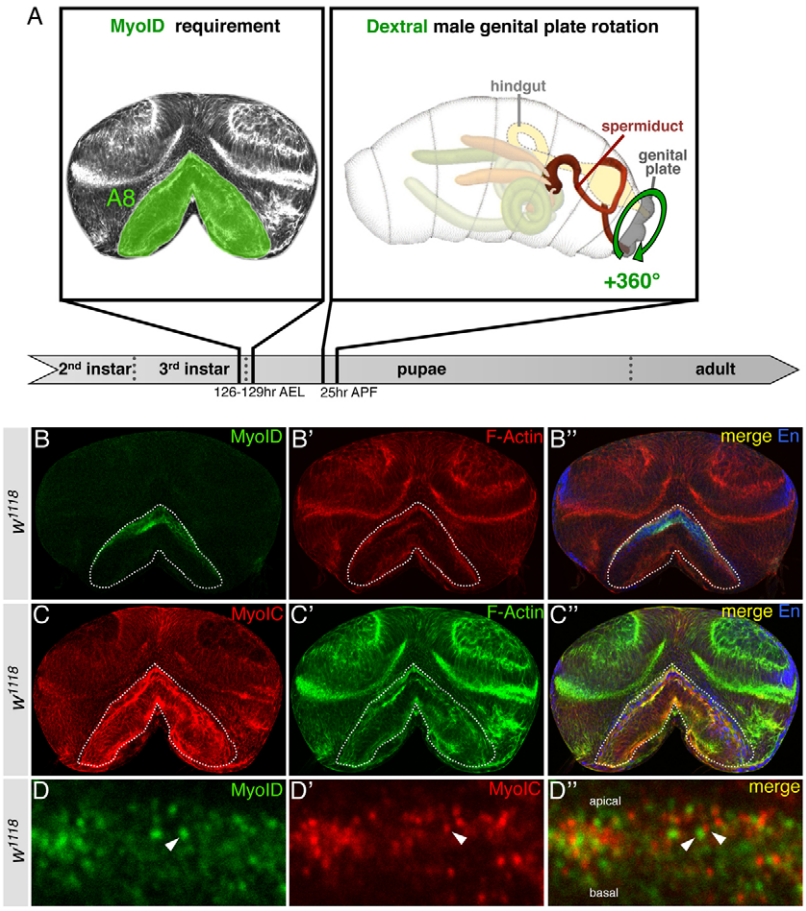

Fig. 1. Looping of genitalia and expression pattern of MyoIC and MyoID. (**A**) Left: Graphic depiction of a third instar larval male genital disc. The A8 segment, in which MyoID activity is required for L/R determination at 126-129 hours after egg laying (AEL), is shaded in green (Speder et al., 2006). Right: Schematic representation [modified from Hartenstein (Hartsenstein, 1993)] of the spermiduct (dark red) looping, and associated 360° clockwise, or dextral, rotation of the male genitalia during pupal stages (green arrow) (Suzanne et al., 2010). APF, after puparium formation. (**B-D″**) Wild-type male genital discs (w^{1118}) stained for MyoID, MyoIC, F-Actin and En. The A8 segment is outlined (dotted line). (B-B″) Expression pattern of MyoIC (red). Engrailed (blue) marks the posterior compartments of the A8, A9 and A10 segments. (C-C″) Expression pattern of MyoID (green). MyoID is expressed exclusively in the A8 segment. (D-D″) Enlargement of A8 cells at the boundary between A9 and A8. MyoID (green) and MyoIC (red) show mutually exclusive localization domains (arrowheads).

Here, we investigate the role of adherens junctions in L/R asymmetry establishment in *Drosophila*. Using targeted genetic invalidation and biochemical approaches, we show that DE-Cadherin (Shotgun – FlyBase) serves as a signalling platform for L/R asymmetry and promotes its implementation through MyoID direct binding and the additional repression of the anti-dextral activity of MyoIC (Myo61F – FlyBase), a closely related unconventional type I myosin. We show that MyoIC antagonizes MyoID and that these myosins have mutually exclusive localization domains at the cell cortex. Altogether, we describe a novel regulatory network of L/R asymmetry establishment through the adherens junction-dependent regulation of two type I myosins, one activating (MyoID) and the other inhibitory (MyoIC).

MATERIALS AND METHODS

Fly strains, genetics and nomenclature

The following mutant strains were used: $myoID^{K2}$ is a *myoID* null allele (Speder et al., 2006); *Df(3L)920* is a deficiency covering the *myoIC* locus (Hegan et al., 2007). Expression of transgenes was carried out using the bipartite Gal4-UAS system (Brand and Perrimon, 1993). The following transgenic lines were used: *UAS::DE-cadherin*^{RNAi} (#103962 from Vienna *Drosophila* RNAi Stock Center); *UAS::DE-Cadherin*, *UAS::DE-Cadherin*^{DN} (a gift from M. Mlodzik, Mount Sinai School of Medicine, NY, USA). The *UAS::myoID*^{RNAi}, *UAS::myoIC*^{RNAi}, *UAS::MyoIC*, *UAS::MyoID*, *UAS::MyoID-GFP* and *UAS::MyoIC-RFP* constructs were generated following standard procedures (Speder et al., 2006) (this study). The following Gal4 driver lines were used: *Abd-B::Gal4*^{LDN} (de Navas et al., 2006), *myoID::Gal4* (NP1548, National Institute of Genetics Stock Center), *hh::Gal4*, *tsh::Gal4*, *arm::Gal4* (Bloomington Stock Center). All crosses were performed at 30°C unless stated otherwise.

To improve readability, the Gal4 driver lines were named after the gene used for Gal4 expression specificity and the '::Gal4' was substituted for '>'. Similarly, UAS constructs were simplified to the sequence expressed and placed after the '>' sign. For example, *UAS::MyoID-GFP; Abd-B::Gal4*^{LDN} becomes *Abd-B>MyoID-GFP*.

Immunostaining of imaginal discs and imaging

We raised new polyclonal antibodies against MyoIC and MyoID. For the generation of anti-MyoIC antibodies, we used for immunization a GST-fusion protein containing the MyoIC-tail residues 765-1026 (PB isoform), and followed the procedure described in Speder et al. (Speder et al., 2006). An anti-MyoID rat polyclonal antibody was generated by Eurogentec against the two following peptides: residues 987-1001 and 824-838. We also used a rabbit polyclonal anti-MyoID, described in Speder et al. (Speder et al., 2006). These antibodies were all used at a 1/50 dilution. Other primary antibodies were polyclonal rat anti-DE-Cadherin (1/50), polyclonal mouse anti-β-catenin (1/50), polyclonal mouse anti-Dlg (1/500) and anti-En (1/100) and were from Developmental Studies Hybridoma Bank. Fluorescent secondary antibodies were Alexa 488, Alexa 546 or Cy5 633 goat anti-rat, anti-rabbit or anti-mouse from Invitrogen (1/400), and phalloidin-TRITC or phalloidin-FITC FluoProbes from Sigma (0.2 µg/ml). We carried out immunostaining according to standard procedures (Speder et al., 2006). For each genotype, 15-20 discs were analysed. Images were captured on a Zeiss LSM 510 META confocal microscope using 40× and 63× objectives. Picture processing was carried out in Adobe Photoshop 7.0 and CS4.

Temperature-shift experiments

The experiments were carried out as described in Speder et al. (Speder et al., 2006) by crossing the *tub::Gal80*^{ts}*; Abd-B::Gal4*^{LDN} and UAS::MyoIC lines or the *myoID::Gal4; tub::Gal80*^{ts} and *UAS::DE-cadherin*^{RNAi} lines. Temperature shifts were performed from 25°C to 29°C and from 29°C to 25°C in a temperature-controlled water bath.

Clonal analysis

myoID^{RNAi} flip-out clones were generated by crossing the *hs-flp; +; UAS::myoID^{RNAi} / SM5-TM6B* to *act[FRT]CD8[FRT]Gal4, UAS::GFPnls* lines. Heat shock was applied for 10 minutes at 34°C at 72-96 hours after egg-laying.

Western blot analysis

One hundred genital discs of each genotype were dissected and lysed in RIPA buffer (1% Triton X-100, 150 mM NaCl, 50 mM Tris-HCl, pH 8) by vortexing. After addition of Laemmli buffer (1×) followed by 5 minutes at 96°C, the whole protein extract was charged on a 10% SDS-PAGE gel. Separated proteins were transferred onto Optitran BA-S 85 reinforced nitrocellulose membranes (Whatman) and detected using HRP Substrate Peroxide Solution (Millipore). Proteins were detected using the following primary antibodies: rat anti-MyoID (1:50), rabbit anti-MyoIC (1:500), rat anti-DE-Cadherin (1:500), polyclonal mouse anti-β-catenin (1:200). Secondary antibodies were: rat, rabbit or mouse anti-HRP from GE Healthcare (1:10,000). For membrane stripping, blots were incubated for 1 hour at 37°C with constant shaking in stripping buffer (0.2 M glycine, 0.1% SDS, 1% Tween, pH 2.2).

Co-immunoprecipitation

Mid-third instar larvae expressing MyoIC-RFP or MyoID-GFP under the control of *arm::Gal4* driver were lysed in lysis buffer (50 mM Tris-HCl, pH 7.5, 150 mM NaCl, 1% Triton X-100, 1 mM $MgCl_2$). Larval extracts (1 mg of protein) were incubated overnight at 4°C with 6 μg of rabbit anti-RFP (Rockland) or rabbit anti-GFP (Sigma-Aldrich) antibodies. The antigen–antibody complex was precipitated with 80 μl of a 50% slurry of proteinA/proteinG Sepharose beads and incubated for 2 hours at room temperature. The beads were recovered by centrifugation for 1 minute at 400 ***g*** and washed four times with lysis buffer. Samples were denatured for 5 minutes at 75°C and loaded onto NuPAGE Novex gel (4%-12% Tris-Glycine, Invitrogen). Enhanced chemiluminescence was used for antibody detection of DE-Cadherin and β-Catenin after blotting on Immobilon-P^{SQ} membrane (Millipore).

RESULTS

MyoIC overexpression causes a situs inversus phenotype

MyoID plays a major role in L/R determination in *Drosophila* (Hozumi et al., 2006; Speder et al., 2006). To test whether other myosins are involved in L/R asymmetry establishment, we systematically expressed RNAi and available overexpression constructs against all known *Drosophila* myosins in the A8 segment of the male genital disc, the genitalia L/R organizer (Table 1), using the UAS-/Gal4 targeting system (Brand and Perrimon, 1993). We found that overexpression of MyoIC leads to a strong situs inversus phenotype, with flies showing sinistral genitalia rotation (Table 1; Table 2, row 4), instead of the wild-type dextral rotation. Interestingly, MyoIC is also a type I unconventional myosin and the closest homologue of MyoID. It was shown previously that upon MyoIC overexpression the direction of embryonic gut looping, an early marker of L/R asymmetry, is inverted (Hozumi et al., 2008; Hozumi et al., 2006). However, depletion of MyoIC activity in the L/R organizer did not affect the rotation of the genitalia which remained wild type (i.e. dextral) (Table 1; Table 2, row 3). We could not observe L/R axis inversion for any of the other *Drosophila* myosins. In some cases, however, their RNAi-mediated silencing led to mild rotation defects without

Table 1. Male genitalia rotation phenotypes associated with silencing or overexpression of *Drosophila* myosins

		Rotation phenotype (%)									
		Abd-B> driver					tsh> driver				
		Dextral		No rotation	Sinistral		Dextral		No rotation	Sinistral	
	Transformant ID‡	Full	Partial		Partial	Full	Full	Partial		Partial	Full
Silencing											
didum (CG2146)	44291	73	27	0	0	0	100*	0	0	0	0
	44292	100	0	0	0	0	20	80	0	0	0
	16902	100	0	0	0	0	21	79	0	0	0
myo10A (CG2174)	37530	100	0	0	0	0	100	0	0	0	0
ninaC (CG 5125)	27360	100	0	0	0	0	66	34	0	0	0
myo 95E (CG5501)	33776	94	6	0	0	0	73	27	0	0	0
	33775	100	0	0	0	0	20	80	0	0	0
	51207	100	0	0	0	0	100*	0	0	0	0
jaguar (CG5695)	37535	87	13	0	0	0	93*	7	0	0	0
	37534	66	34	0	0	0			lethal		
myo 28B1 (CG6976)	37531	87	13	0	0	0	100*	0	0	0	0
myoID* (CG7438)*		**0**	**0**	**30**	**69**	**1**	**0**	**0**	**0**	**55**	**45**
crinkled (CG7595)	9265	100	0	0	0	0	87	13	0	0	0
myoIC (CG9155)	101033	100	0	0	0	0	100	0	0	0	0
dachs (CG10595)	12555	100	0	0	0	0	100*	0	0	0	0
	12556	100	0	0	0				lethal		
zipper (CG15792)	7819	0	100	0	0	0			lethal		
mhc (CG17927)	7164	92	8	0	0	0			lethal		
Overexpression											
Jaguar		87	13	0	0	0	0	0	0	0	0
MyoID		100	0	0	0	0	100	0	0	0	0
MyoIC		**0**	**0**	**91**	**9**	**0**	**0***	**0**	**0**	**20**	**80**
Zipper		34	66	0	0	0	0	0	0	0	0

*Flies were first raised at 25°C to avoid lethality at early developmental stages and then shifted to 30°C from day 4 on.
**For further details, see Speder et al. (Speder et al., 2006).
‡Transformant ID corresponds to the RNAi-line reference at the VDRC.

Table 2. Male genitalia rotation phenotypes of various MyoIC, MyoID or DE-Cadherin genetic conditions

		Rotation phenotype (%)						
		Dextral				No rotation	Sinistral	
			Partial					
		Full	+359°/+181°	+180°/+91°	+90°/+1°		Partial	Full
MyoID–MyoIC interaction								
1	*myoID^{k2}*	0	0	0	0	0	23	77
2	*myoID>MyoID*	100	0	0	0	0	0	0
3	*myoID>myoIC^{RNAi}/Df(3L)920*	100	0	0	0	0	0	0
4	*myoID>MyoIC***	0	0	0	0	0	0	100
5	*Gal80^{ts};myoID>myoID^{RNAi}, myoIC^{RNAi}**	0	0	0	0	0	100	0
6	*myoID^{k2}; Df(3L)920, Abd- B>myoIC^{RNAi}, dicer2*	0	0	0	0	0	85	15
7	*myoID>MyoID-GFP, MyoIC-RFP*	100	0	0	0	0	0	0
8	*myoID>MyoIC-RFP*	0	0	0	0	47	53	0
9	*myoID>MyoIC-RFP, UAS-lacZ* (control)	0	0	0	0	87	13	0
10	*myoID>MyoID-GFP*	100	0	0	0	0	0	0
11	*myoID>MyoID-GFP, UAS-lacZ* (control)	100	0	0	0	0	0	0
DE-Cadherin–myosin interaction								
12	*w^{1118} x DE-cad.^{RNAi}* (control)	100	0	0	0	0	0	0
13	*Abd-B>DE-cad.^{RNAi}, dicer2*	0	0	8	64	32	0	0
14	*myoID>DE-cad.^{RNAi}****	0	0	0	80	20	0	0
15	*myoID>DE-cad.^{RNAi}, myoIC^{RNAi}****	0	0	47	47	6	0	0
16	*myoID>DE-cad.^{RNAi}, UAS-lacZ* (control)***	0	0	10	75	15	0	0
17	*myoID>myoIC^{RNAi}, UAS-lacZ* (control)	100	0	0	0	0	0	0
18	*myoID>DE-Cad.*				lethal			
19	*Abd-B>DE-Cad.*	47	53			0	0	0
20	*Abd-B>DE-cad.^{RNAi}, dicer2**	0	2	64	34	0	0	0
21	*Abd-B>myoID^{RNAi}*, dicer2**	0	0	0	0	40	60	0
22	*Abd-B>DE-cad.^{RNAi}, myoID^{RNAi}, dicer2**	0	0	13	19	68	0	0

*Flies were first raised at 25°C to avoid lethality at early developmental stages and then shifted to 30°C from day 4 on.
**Flies were raised at 25°C owing to lethality at 30°C.
***Phenotype of pharate adults

affecting directionality, thus probably affecting the mechanical aspect of the rotation process (for details, see Table 1). These results indicate that only type I myosins have a specific role in L/R determination in *Drosophila*.

MyoIC has anti-dextral activity

Two models can explain the sinistral phenotype caused by MyoIC overexpression: (1) MyoIC might act as a sinistral determinant, overriding the dextral activity of MyoID, or (2) MyoIC might act as an anti-dextral factor, inhibiting MyoID activity. If MyoIC harbours a sinistral activity, then the simultaneous loss of dextral (MyoID) and potentially sinistral (MyoIC) functions should lead to a 'no-rotation' phenotype. To test whether MyoIC is a sinistral determinant, we generated double mutant flies lacking both MyoID and MyoIC activities. In these flies, we observe a clear sinistral phenotype (Table 2, rows 5, 6), which is identical to the loss of MyoID alone. This result indicates that MyoIC does not bear an independent sinistral activity, but rather acts as a negative regulator of MyoID activity and, therefore, exerts an anti-dextral function.

To gain better insights into the MyoIC-MyoID interaction, we generated antibodies against each protein (see Materials and methods) and analysed their expression pattern in wild-type discs. MyoIC was expressed in the entire male genital disc and was enriched in the A8 segment (Fig. 1C), overlapping with the A8-specific expression of MyoID (Fig. 1B). We performed co-immunostaining analysis to determine the intracellular localization of both MyoID and MyoIC. Although both myosins were detected in the same cells, careful analysis revealed that at the cellular level MyoID and MyoIC have mutually exclusive cortical localization patterns (Fig. 1D).

In an effort to characterize the anti-dextral activity of MyoIC, we analysed the intracellular localization of both myosins in a MyoIC gain-of-function condition and compared it with the wild-type situation (Fig. 2A). We observed a fully penetrant reduction of MyoID signal (Fig. 2B), which is consistent with the sinistral phenotype of these flies and indicates a loss of MyoID activity. Reciprocally, MyoID overexpression induced a decrease of MyoIC signal (Fig. 2C). The wild-type dextral phenotype of these MyoID overexpressing flies is consistent with the wild-type dextral phenotype of MyoIC loss-of-function flies (see above; Table 2, row 3). From these data, we conclude that MyoIC and MyoID are mutually inhibiting each other's localization to specific cortical domains.

MyoID overexpression rescues the MyoIC-induced situs inversus phenotype

To test whether MyoID expression levels could counteract the dominant effect of MyoIC overexpression, MyoID and MyoIC were co-overexpressed in the A8 segment. In this context, we observed a wild-type dextral rotation phenotype. A dilution effect of the Gal4 activator was ruled out using a *UAS::lacZ* control overexpressed with either myosin (Table 2, rows 8-11). These results thus indicate that MyoID overexpression is able to rescue MyoIC overexpression (Table 2, row 7). Accordingly, we detected a colocalization of MyoID and MyoIC at the membrane and in the cytoplasm (Fig. 2D), indicating that MyoID is no longer excluded by MyoIC and reoccupies its wild-type cortical domain. These results show that the observed MyoIC-induced situs inversus phenotype is linked to the loss of MyoID localization and activity

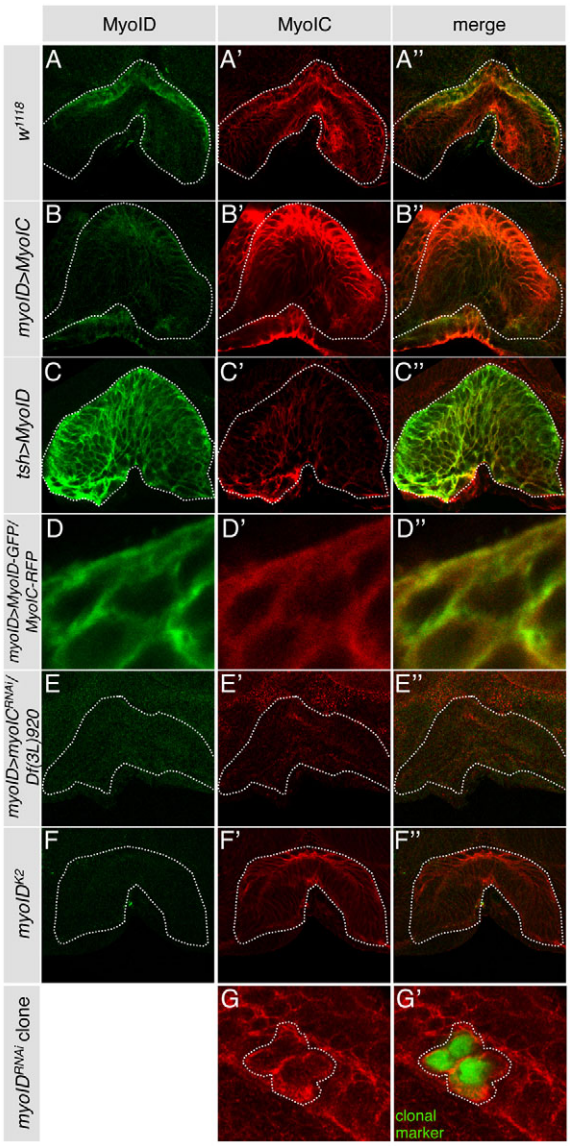

Fig. 2. Immunofluorescence analysis of MyoID and MyoIC localizations in loss- and gain-of-function conditions. (**A-F″**) Male genital discs stained for MyoID (green) and MyoIC (red). The dotted lines outline the A8 segment. The genetic conditions are: (A) *w*^{1118} (wild-type), (B) *myoID::Gal4; UAS::MyoIC*, (C) *tsh::Gal4; UAS::MyoID*, (D) *myoID::Gal4 / UAS::MyoID-GFP; UAS::MyoIC-RFP / +*, (E) *myoID::Gal4 / myoIC*^{RNAi}*; Df(3L)920 / +* and (F) *myoID*^{k2}. (**G**,**G′**) Flip-out clones marked with GFP expressing *UAS::myoID*^{RNAi} generated in male genital discs stained for MyoIC (red). MyoIC expression appears similar in the clone cells and surrounding wild-type tissue. Dotted lines outline the clone cells.

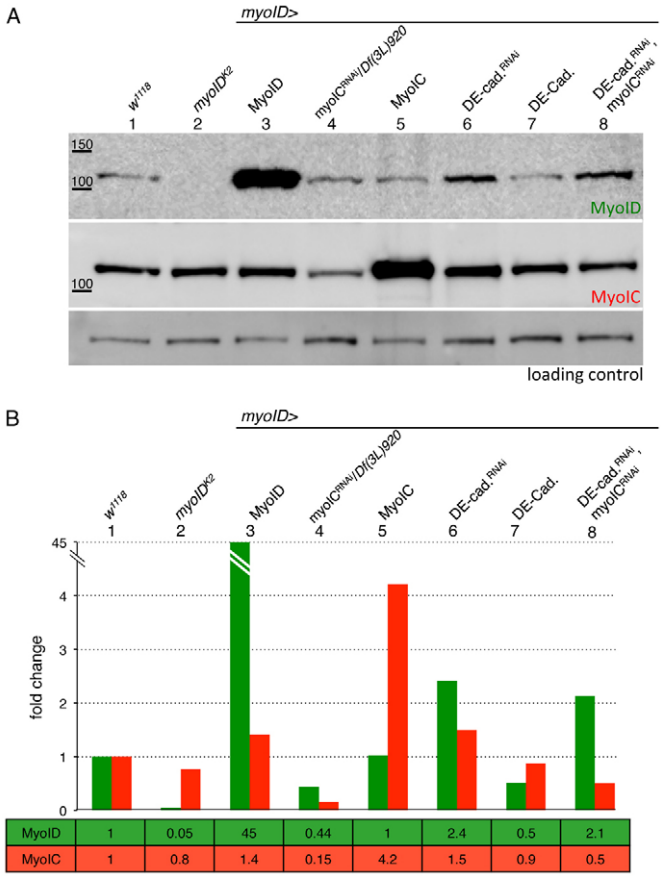

Fig. 3. MyoID and MyoIC protein level in various genetic conditions. (**A**,**B**) Western blot analysis (A) and quantification (B) of MyoID and MyoIC protein levels in *w*^{1118} (1), *myoID*^{k2} (2), and *myoID::Gal4*-driven *UAS::MyoID* (3), *UAS::myoIC*^{RNAi} */ Df(3L)920* (4), *UAS::MyoIC* (5), *UAS::DE-Cadherin* (6), *UAS::DE-cadherin*^{RNAi} (7) and *UAS::DE-cadherin*^{RNAi} */ UAS::myoIC*^{RNAi} (8) male genital discs.

in the A8 segment cells. Furthermore, it shows the importance of the MyoID-MyoIC protein balance for proper L/R asymmetry establishment.

Loss of myosin activity is not due to protein degradation

To gain a further understanding of the molecular nature of the mutual inhibition between MyoIC and MyoID, we investigated whether the protein levels of either myosin were changed upon overexpression of the other myosin. To address this question, we performed western blot analysis on dissected genital discs in which the myosin protein or RNAi overexpression is limited to the A8 segment. The control lanes show that MyoID or MyoIC protein levels were increased upon overexpression, thus validating the approach (Fig. 3A, lane 3, upper panel and lane 5, middle panel). The differences of endogenous expression domains of MyoID (restricted to the A8 segment) and MyoIC (expressed in all genitalia segments A8, A9 and A10) probably account for the 45-fold change of MyoID and only fourfold change of MyoIC observed upon overexpression. Surprisingly, we found that MyoID protein concentration remains unchanged upon MyoIC overexpression (Fig. 3A, lane 5, upper panel). Reciprocally, upon MyoID overexpression MyoIC protein level was only slightly altered (Fig. 3A, lane 3, middle panel).

Therefore, neither myosin is degraded upon overexpression of the other myosin, although they became undetectable by immunohistochemistry (Fig. 2B,C). The loss or reduction of antigen detection could be due to, first, a conformational change of the protein or concealment of the epitopes in a protein complex, or, second, the displacement of the protein from the membrane into the cytoplasm, leading to its dilution. Therefore, MyoID function assessment should not be limited to its detectability by immunofluorescence but rather on the genitalia rotation phenotype.

Loss of MyoIC does not affect MyoID function, but modifies MyoID organization

To characterize further the interaction between MyoIC and MyoID, we analysed the impact of the loss of one of the myosins on the expression and localization of the other. In MyoIC loss of function, we observed a decreased MyoID signal (Fig. 2E) and a concomitant twofold reduction of MyoID protein by western blot (Fig. 3A, lane 4). However, the wild-type dextral phenotype seen in this condition (Table 2, row 3) suggests that half a dose of MyoID protein is sufficient for its function (MyoID/MyoIC ratio>1). Nevertheless, MyoID intracellular localization and/or organization are changed, as suggested by the reduced antibody detection (Fig. 2E).

By contrast, MyoID loss of function had no strong effect on MyoIC expression, as neither MyoIC localization nor protein level was altered (Fig. 2F and Fig. 3A, lane 2, middle panel). This result was confirmed cell-autonomously with *myoID*^{RNAi}-expressing clones (Fig. 2G).

In summary, MyoID remains active upon MyoIC loss of function and becomes inactive when MyoIC protein levels are increased or, more generally, when MyoIC levels are much above the levels of MyoID (MyoID/MyoIC ration <<1). In wild-type flies, MyoID is able to act and to promote dextral determination in spite of MyoIC presence. MyoID is not equally able to affect MyoIC localization and expression. These results confirm the anti-dextral function of MyoIC as an antagonist of MyoID**.**

DE-Cadherin is required for L/R asymmetry

MyoID has been shown to interact physically and to colocalize with the adherens junction component β-Catenin (Speder et al., 2006). We thus investigated whether adherens junctions could act as a regulatory signalling platform for MyoID function during L/R asymmetry establishment. To test this hypothesis, we first silenced the adherens junction component DE-Cadherin specifically in the A8 segment. This depletion resulted in a highly penetrant no-rotation (0°) and close-to-no-rotation (1-90°) phenotype (Table 2, row 13). Interestingly, immunofluorescence analysis revealed a concomitant loss of MyoID signal in this context (Fig. 4B), consistent with the no-rotation phenotype and a loss of MyoID activity. In stronger conditions of DE-Cadherin depletion, a close to fully penetrant no-rotation phenotype was observed, suggesting that no-rotation could represent the end phenotype of a full DE-cadherin loss of function.

Furthermore, we also observed an increased MyoIC signal upon *DE-cadherin* silencing (Fig. 4B), suggesting that DE-Cadherin negatively regulates MyoIC. Similar results were obtained upon overexpression of a dominant-negative form of DE-Cadherin (DE-Cad.^{DN}) in the posterior compartment of all the genital disc segments (A8, A9, A10), indicating that the regulation of MyoIC by DE-Cadherin is not specific to the A8 segment (Fig. 4C). These results show that a reduction in DE-Cadherin leads to an increase in MyoIC expression and a concomitant reduction in MyoID immunodetection.

DE-Cadherin also promotes MyoID function through repression of MyoIC

Strikingly, the effect of DE-Cadherin reduction led to a decrease in MyoID signal in the A8 segment (Fig. 4B) and a loss of MyoID activity leading to rotation defects (Table 2, rows 13, 14). Furthermore, upon DE-Cadherin reduction we observed an increased MyoIC signal by immunohistochemistry and an increase in MyoIC protein level by western blot (Fig. 3A, lane 6, middle panel). In this context, MyoID protein level is also increased, suggesting that DE-cadherin controls the protein level of both myosins.

To test whether the increase in MyoIC level impacts on the rotation defects of DE-Cadherin depletion, we examined the effect of the absence of both DE-Cadherin and MyoIC on MyoID and on genitalia rotation. In the double *DE-cadherin*, *myoIC* mutant context, the rotation defects are shifted towards a more wild-type phenotype, not due to the mere Gal4 dilution (Fig. 4E; Table 2, rows 14-17). The level of MyoID protein was also slightly reduced, consistent with MyoIC reduction as previously observed (Fig. 3,

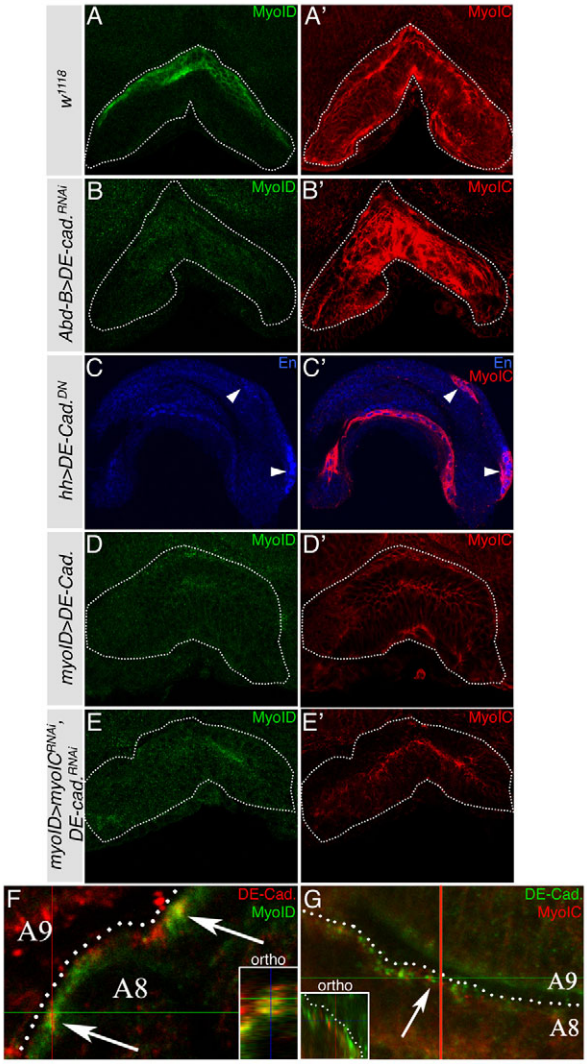

Fig. 4. DE-Cadherin regulates MyoIC and MyoID expression. (**A-E′**) Immunofluorescence analysis of MyoID (green) and MyoIC (red) in wild-type, *w*^{1118} (A), DE-Cadherin loss-of-function, *Abd-B::Gal4*^{LDN} / *UAS::DE-cadherin*^{RNAi} (B), *hh::Gal4* / *UAS::DE-cadherin*^{DN} (C), DE-Cadherin overexpression *myoID::Gal4* / *UAS::DE-cadherin* (D) and DE-Cadherin and MyoIC loss-of-function *myoID::Gal4; UAS::DE-cadherin*^{RNAi} / *UAS::myoIC*^{RNAi} (E) conditions. The dotted lines outline the A8 segment. For each genotype, 15-20 discs were analysed. Arrowheads indicate the cells expressing *DE-cadherin*^{DN}. (**F**,**G**) DE-Cadherin colocalizes with MyoID (F), but not with MyoIC (G). Dotted line indicates boundary between A8 and A9. Arrows indicate DE-cadherin-rich spots. Insets show orthogonal plane of the red line, giving the view along the cell apico-basal axis.

lane 4). However, MyoID remained higher than normal upon *DE-cadherin* silencing, suggesting that DE-Cadherin regulates MyoID protein level through an unknown and MyoIC-independent mechanism. Additionally, MyoID was not detected by immunohistochemistry (Fig. 4E) as in the *myoIC* mutant context (Fig. 2E). These results suggest that both the depletion of DE-Cadherin and the increase in MyoIC contribute to the final genitalia rotation defects in the DE-Cadherin depletion context. Thus, DE-Cadherin appears to have two effects on L/R asymmetry: first, promoting MyoID activity and second, repressing MyoIC inhibition (Fig. 7A).

We tested this model further by increasing *DE-cadherin* dosage. Overexpression of DE-Cadherin in the A8 segment did not affect direction of genitalia rotation, which is dextral (Table 2, row 19), indicating that MyoID functions normally. However, MyoIC signal appeared to be strongly decreased (Fig. 4D, compare with wild type in 4A), suggesting a repression of MyoIC by DE-Cadherin. Consistent with the increase of both myosins in *DE-cadherin* loss-of-function conditions (Fig. 3A,B, lane 6), both myosin protein levels were reduced upon DE-Cadherin overexpression (Fig. 3A,B, lane 7, middle panel). It is important to note that in these conditions the silencing is restricted to the small A8 segment, but the contribution of DE-Cadherin and MyoIC in the other segments is not affected, therefore minimizing the effect observed on the western blot. Thus, DE-Cadherin indirectly increases MyoID activity further by repressing MyoIC specifically in the A8 segment.

MyoID was not detectable by immunohistochemistry in the DE-Cadherin overexpression context (Fig. 4D), and its protein level was reduced (Fig. 3A, lane 7, upper panel). Nevertheless, in this context MyoID level is sufficient for proper L/R establishment, owing to the strong decrease in MyoIC (and a favourable MyoID/MyoIC ratio of ~0.5, equivalent to a heterozygous situation for *myoID*), thus consistent with our previous findings in the direct MyoIC silencing conditions (Table 2, row 3; Fig. 2E).

Temporal requirement for DE-Cadherin, MyoIC and MyoID in L/R asymmetry

MyoID activity in directing dextral L/R asymmetry is temporally restricted and only required for 3 hours before pupariation (Speder et al., 2006). To test whether DE-Cadherin, MyoIC and MyoID have synchronous functions in L/R asymmetry, we made use of the temperature-dependent TARGET gene expression system (McGuire et al., 2004) to switch on or off the overexpression of MyoIC or the depletion of DE-Cadherin in the A8 segment at different developmental stages.

The overexpression of MyoIC shows that MyoIC anti-dextral activity takes place during days 6-7 of development and overlaps with the dextral determinant function of MyoID (Fig. 5A) (Speder et al., 2006). Interestingly, the temporal requirement for DE-Cadherin appeared to be broader between days 4-9 of development (Fig. 5B). Thus, the time window of DE-Cadherin function in L/R asymmetry overlaps with the activity peaks of MyoID and MyoIC (Fig. 5A) (Speder et al., 2006). The wider time window for DE-Cadherin can be explained by the applied method, which depends on the half-life of the mRNA and protein. Additionally, reduced DE-Cadherin might not only affect L/R determination at day 6 but also affect cell adhesion and tissue mechanics during the actual rotation of the genitalia at a later stage of morphogenesis. To distinguish between these temporally separate functions, we performed double temperature-shift experiments to silence *DE-cadherin* for short periods of 8 hours during development to narrow

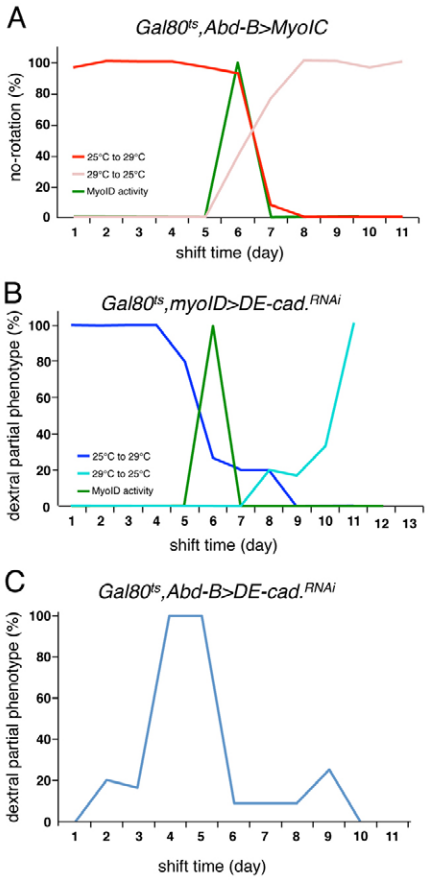

Fig. 5. Temporal requirement for MyoID, MyoIC and DE-Cadherin. (**A-C**) Temperature-shift experiments to determine the temporal window for MyoIC (A) and DE-Cadherin (B,C) requirement in L/R asymmetry establishment. The temporal functional requirement for MyoID is shown in green as described by Speder et al. (Speder et al., 2006). (A) Shift from restrictive to permissive (red) and permissive to restrictive (pink) temperature for MyoIC overexpression. (B) Shift from restrictive to permissive (dark blue) and permissive to restrictive (light blue) temperature for DE-Cadherin activity. (C) Double shift experiment. The flies were shifted from restrictive to permissive temperature for 8 hours at different times of development.

down DE-Cadherin temporal requirement. Using this approach, we show two peaks of DE-Cadherin requirement, the first overlapping with L/R determination and the second with the asymmetric rotation of the genitalia (Fig. 5C). These results suggest an uncoupling of DE-Cadherin functions in L/R determination at day 6, together with MyoID, and in the later genitalia morphogenesis and rotation independently of MyoID. The overlap at day 6 between the temporal functional windows of DE-Cadherin, MyoIC and MyoID is consistent with a synergistic effect of these proteins for L/R determination.

MyoIC prevents the essential interaction between MyoID and adherens junction components

To understand the interaction between DE-Cadherin and type I myosins further, we performed immunofluorescence analysis of wild-type discs and examined the localization of the three proteins. We found that MyoID colocalizes with DE-Cadherin (Fig. 4F), which is consistent with the earlier reported colocalization of MyoID with β-Catenin (Speder et al., 2006). By contrast, DE-

Cadherin did not colocalize with MyoIC (Fig. 4G), which is consistent with an inhibition of MyoIC by DE-Cadherin and our finding of mutually exclusive MyoIC and MyoID cortical localization domains (Fig. 1D).

To characterize the interactions between the adherens junction and both myosins, we performed co-immunoprecipitation experiments from larvae expressing either MyoID-GFP or MyoIC-RFP. As suggested by immunofluorescence analyses and previous results (Speder et al., 2006), β-Catenin could be co-immunoprecipitated with MyoID-GFP from larval extracts (Fig. 6A, lane 1). By contrast, β-Catenin and MyoIC-RFP did not show any interaction (Fig. 6A, lane 2). Furthermore, we showed a novel interaction between MyoID and DE-Cadherin. Indeed, DE-Cadherin co-immunoprecipitated with MyoID but not MyoIC (Fig. 6A′, lanes 1 and 2). Interestingly, both the interactions between MyoID and β-Catenin and MyoID and DE-Cadherin were abolished upon addition of MyoIC-RFP, leading to a strong reduction in, or even absence of, DE-Cadherin, and β-Catenin co-immunoprecipitated with MyoID-GFP (Fig. 6A,A′, lane 3). Therefore, the presence of MyoIC in the protein extracts is sufficient to disrupt the physical interaction between MyoID and the adherens junction components DE-Cadherin and β-Catenin, both in vivo and in vitro.

Taken together, these results suggest that the interactions between MyoID and the adherens junction components, which are inhibited by the antagonist MyoIC, are essential for MyoID function (Fig. 6D).

Other adherens junction components similarly affect myosin function

To support our in vitro data showing an interaction between MyoID and both DE-cadherin and β-Catenin (Fig. 6A) and a model in which the adherens junction acts as a myosin function regulating platform, we silenced other adherens junction components and looked for rotation defects and myosin's localization. Depletion of either α- or β-Catenin in the L/R organizer led to dextral partial phenotypes (Table 3, rows 1-5), whereas stronger mutant conditions using stronger drivers or a combination of RNAi constructs to deplete either catenin together with DE-Cadherin led to lethality (Table 3, rows 6-10).

Interestingly, staining of α- or β-Catenin-depleted genital discs for MyoIC and MyoID showed an increase in MyoIC and a loss of MyoID signal, identical to our observation for *DE-cadherin* silencing (Fig. 6B,C).

These results further support the hypothesis that the adherens junction acts as a platform for myosin function required for L/R asymmetry establishment.

Planar cell polarity genes and *Drosophila* inversin homologue *diego* are not implicated in genitalia directionality

The mouse inversin (*Inv*) and *Drosophila* myoID are to date the only two known situs inversus genes. Inv was found to act as a switch between canonical and non-canonical Wnt signalling. Inv inhibits the canonical Wnt signalling through targeting Dishevelled (Dsh) to degradation (Simons, 2005). Diego, the *Drosophila* homologue of inversin, is a component of the non-canonical Wnt signalling pathway responsible for planar polarization. Therefore, we investigated whether disruption of the planar cell polarity (PCP) pathway, and especially Diego, affects L/R asymmetry in genitalia rotation. To this end, we expressed RNAi against most described PCP genes involved in the PCP pathway into the A8 segment of the genital disc and scored rotation phenotypes (supplementary material Table S1). Several PCP genes, including *diego*, showed dextral partial rotation defects, although none caused an inversion of directionality or a no-rotation phenotype. The partial rotation defects observed are likely to be due to polarization defects that affect the rotation process per se. Altogether, these results indicate that *diego* and other PCP genes do not play a major role in LR directionality in *Drosophila*.

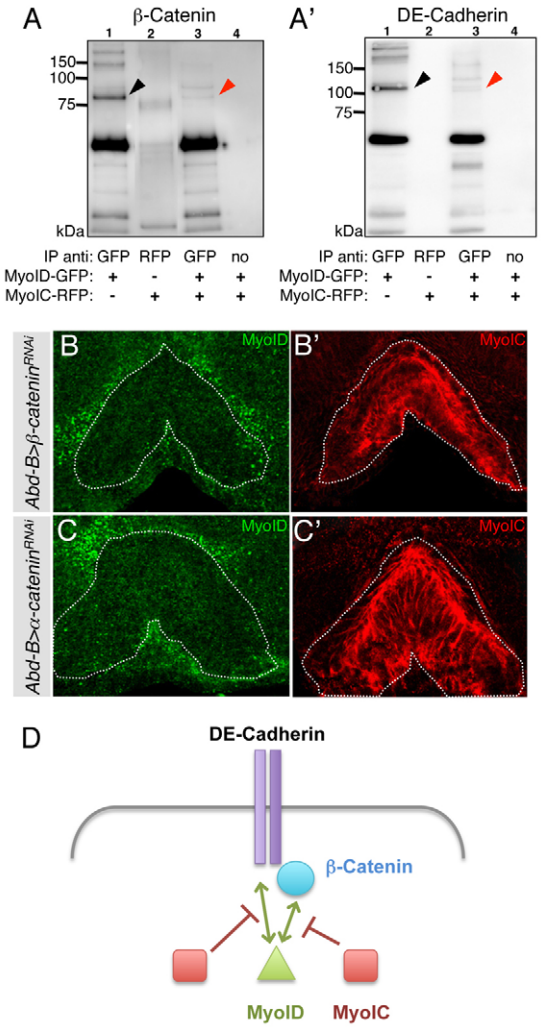

Fig. 6. MyoIC disrupts MyoID interaction with adherens junction components. (**A**,**A′**) Co-immunoprecipitation experiments using larval extracts expressing MyoID-GFP or MyoIC-RFP. Adherens junction component β-Catenin (A) and DE-Cadherin (A′) are co-immunoprecipitated with MyoID-GFP (A,A′, lane 1, black arrowheads) but not with MyoIC-RFP (A,A′, lane 2). Both the interactions between MyoID-GFP and β-Catenin or DE-Cadherin are disrupted in presence of elevated MyoIC-RFP concentrations (A,A′, lane 3, red arrowheads). Control lane (lane 4, no antibody used for immunoprecipitation) is used for background signal. (**B-C′**) β-Catenin (*Abd-B::Gal4^{LDN} / UAS::β-catenin^{RNAi}*), (B) or α-Catenin (*Abd-B::Gal4^{LDN} / UAS::α-catenin^{RNAi}*), (C) depleted male genital discs stained for MyoID (green) and MyoIC (red). Silencing of *α-catenin* or *β-catenin* in the A8 segment leads to a loss of MyoID signal (B,C) and an increase in MyoIC signal (B′,C′). Dotted line outlines the A8 segment. (**D**) Schematic of DE-Cadherin, β-Catenin, MyoIC and MyoID interactions.

Table 3. Male genitalia rotation phenotypes associated with α- and β-Catenin silencing

		Rotation phenotype				
		Dextral		No rotation	Sinistral	
		Full	Partial		Partial	Full
1	*myoID>β-catenin^{RNAi}*	67	33	0	0	0
2	*Abd-B>β-catenin^{RNAi}, Dicer2*	13	87	0	0	0
3	*tsh>β-catenin^{RNAi}*			lethal		
4	*myoID>α-catenin^{RNAi}*	54	46	0	0	0
5	*Abd-B>α-catenin^{RNAi}, Dicer2*	0	100	0	0	0
6	*tsh>α-catenin^{RNAi}*			lethal		
7	*myoID>β-catenin^{RNAi}, DE-cad.^{RNAi}*			lethal		
9	*myoID>α-catenin^{RNAi}, DE-cad.^{RNAi}*			lethal		
10	*Abd-B>α-catenin^{RNAi}, Dicer2, DE-cad.^{RNAi}**	0	77	23	0	0

α-*catenin* or β-*catenin* activities were depleted either alone or combined to *DE-cadherin* depletion and the male genitalia rotation phenotypes were scored.
*Inner and outer deformation of the genitalia.

DISCUSSION

Although several L/R molecules and signalling pathways have been identified in vertebrates, the molecular mechanisms underlying stereotyped L/R asymmetry establishment in invertebrates are largely unknown (Speder et al., 2007). Recently, an actin-based molecular motor, the unconventional type ID myosin, was identified as a L/R determinant in *Drosophila*, sufficient to orient the L/R axis (Hozumi et al., 2006; Speder et al., 2006). In this study, we describe a novel regulatory network controlling MyoID activity that is adherens junction dependent and can be antagonized by MyoIC, the closest homologue of MyoID.

DE-Cadherin contributes dually to L/R establishment by promoting MyoID function and repressing MyoIC antagonism

We show that DE-Cadherin has a dual role in promoting MyoID activity. DE-Cadherin directly stabilizes MyoID at the adherens junctions and inhibits the antagonistic activity of MyoIC, thus eliciting MyoID function. We show further that MyoID activity and organization are dependent on the level of MyoIC protein. In MyoIC gain of function, MyoID intracellular pattern is modified with a reduced overall signal and the protein level remains unchanged (Fig. 2B; Fig. 3, lane 5). In MyoIC loss of function, MyoID is not detected by immunohistochemistry and the protein level measured by western blot is reduced (Fig. 2E; Fig. 3, lane 4). Nevertheless, in MyoIC loss of function, sufficient MyoID activity remains as confirmed by the wild-type rotation phenotype (Table 2, row 3). Thus, MyoID activity is only impaired when MyoIC is in large excess (MyoID/MyoIC ration <<1; Fig. 2B, Table 2, row 4).

It is important to note that these results were obtained through two independent approaches, either by direct modulation of MyoIC expression levels (Fig. 2B,E) or indirectly by affecting *DE-cadherin* (Fig. 4B,D), silencing of which in the A8 segment leads to an increase of MyoIC (and of MyoID) levels (Fig. 3). These results indicate that DE-Cadherin negatively regulates both MyoID

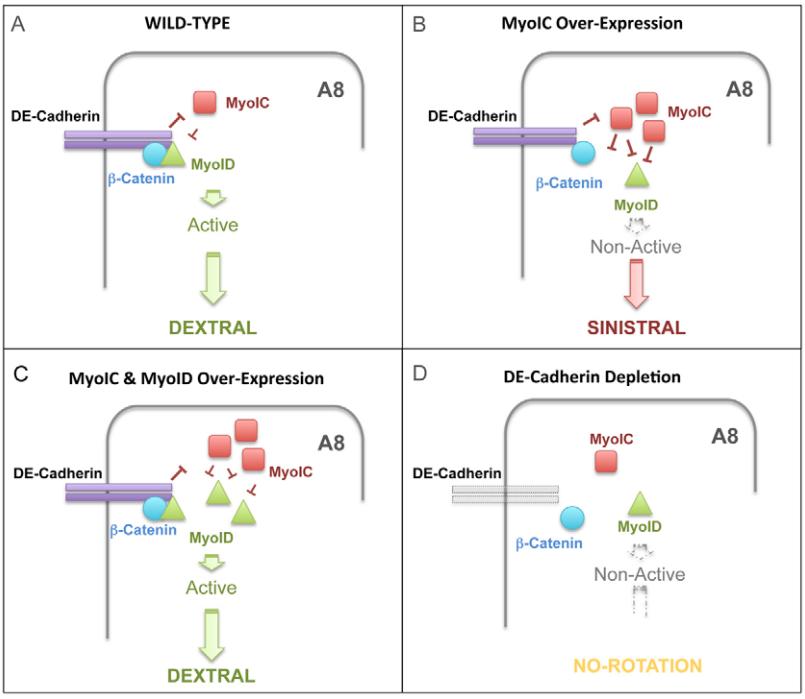

Fig. 7. The adherens junction serves as a signalling platform to establish *Drosophila* L/R asymmetry. (**A-D**) Schematic of the interactions between DE-Cadherin (purple), β-Catenin (blue), MyoID (green) and MyoIC (red) during L/R asymmetry establishment in various genetic contexts. (A) Wild type. At the adherens junction, MyoID association with β-Catenin is stabilized by DE-Cadherin through repression of MyoIC antagonistic function. Thus, MyoID is active and triggers dextral L/R development. (B) Upon MyoIC overexpression, MyoID association with β-Catenin is disrupted, impairing MyoID L/R function, and thus leading to sinistral L/R development. (C) MyoID overexpression can compensate for that of MyoIC. MyoID association with β-Catenin is restored eliciting normal dextral L/R development. (D) In absence of DE-Cadherin, MyoID cannot act to conduct dextral L/R development; neither can the sinistral pathway leading to no-rotation phenotype.

and MyoIC levels. Taken together, these data indicate that DE-Cadherin controls both the L/R determinant MyoID and its repressor MyoIC activity and protein levels (Fig. 3, lanes 6, 7; Fig. 4D).

DE-Cadherin functions in *Drosophila* L/R asymmetry

Specific depletion of DE-Cadherin in the A8 segment, the L/R organizer (Speder et al., 2006), leads to a no-rotation phenotype. Could stronger depletion of the adherens junction components leads to a sinistral phenotype? In other words, does DE-Cadherin depletion also affect sinistral development or pathway, which is taking over in absence of MyoID? To tackle this question, we depleted both DE-Cadherin and MyoID. We find that, unlike the sole depletion of MyoID that leads to a majority of sinistral flies, the double depletion leads to a majority of non-rotated flies (Table 2, rows 20-22). These data therefore indicate that DE-Cadherin acts both on the dextral (MyoID-dependent) and on the sinistral pathways, making it a general regulator of L/R asymmetry in flies.

Adherens junctions have previously been connected to MyoID-mediated L/R asymmetry establishment through biochemical analysis, which identified a physical interaction between the MyoID-tail domain and β-Catenin in vitro (Speder et al., 2006). In this study, we show a role of the adherens junction in the *Drosophila* L/R pathway and place the adherens junction component DE-Cadherin as a regulator of both unconventional myosins MyoIC and MyoID. DE-Cadherin dually promotes MyoID and β-Catenin association at the adherens junctions and inhibits the antagonistic function of MyoIC (Fig. 7A). Indeed, we observe a partial colocalization of MyoID and DE-Cadherin and the concomitant exclusion of MyoIC from the adherens junction (Fig. 4F,G). Further supporting this model is the additional biochemical evidence that MyoID, but not MyoIC, can directly interact with DE-Cadherin and β-Catenin in vitro (Fig. 6). Excess of MyoIC is able to disrupt this interaction both in vivo and in vitro, leading to MyoID loss-of-function phenotypes (Fig. 7B). This disruption can be rescued by MyoID overexpression (Fig. 7C). We propose that MyoID L/R function depends on its physical interaction with adherens junction through both β-Catenin and DE-Cadherin (Fig. 7A). Upon adherens junction reduction, MyoID does not associate with β-Catenin, MyoIC is no longer repressed and in turn inhibits MyoID activity, leading to L/R defects (Fig. 7D). Finally, the temporal synchrony of MyoID, MyoIC and DE-Cadherin requirement in genitalia rotation implies a concomitant activity of these proteins in L/R establishment.

Interestingly, MyoIC has previously been reported to affect L/R looping of the embryonic gut, another marker of L/R asymmetry in *Drosophila* (Hozumi et al., 2006). It was shown that MyoIC overexpression also causes fully penetrant embryonic gut inversion (Hozumi et al., 2006). Thus, the antagonistic function of MyoIC appears to be conserved in *Drosophila* L/R tissues. Furthermore, it was recently shown that DE-Cadherin is required for L/R asymmetry establishment of the *Drosophila* hindgut (Taniguchi et al., 2011). The dextral curving of the hindgut was lost in a *myoID* and *DE-cadherin* mutant background accompanied by a loss of L/R biased asymmetric cell shape and a differential DE-Cadherin localization. The authors suggest that both factors are implicated in the creation of asymmetric cortical tension prior to asymmetric curving of the hindgut. Taken together, these data indicate that the *Drosophila* L/R tissues, hindgut and genitalia, show a similar dependency on adherens junction and type I unconventional myosins for L/R determination.

Is the role of adherens junctions in L/R asymmetry establishment conserved among species?

Interestingly, despite the apparent differences between vertebrates and invertebrates mechanisms of L/R asymmetry establishment (Speder et al., 2007), a common theme can be found in the only two molecularly described situs inversus genes to date. In addition to *myoID*, the mouse inversin gene also causes constant L/R axis inversion in homozygous mutants (Yokoyama et al., 1993). Interestingly, the inversin protein was shown to co-precipitate with β-catenin and N-cadherin and to localize to the adherens junction of polarized epithelial cells (Nurnberger et al., 2002). Therefore, both situs inversus proteins interact with β-catenin and associate with adherens junction molecules, such as N- or E-cadherin. Additionally, N-cadherin was reported to play a role in L/R asymmetry establishment in chicken, as N-cadherin absence at the Hensen's node leads the randomization of L/R asymmetry (Garcia-Castro et al., 2000), similar to our results showing a role of DE-Cadherin in L/R determination in *Drosophila*. The *Drosophila* inversin homologue *diego* belongs to the planar cell polarity gene family. Depletion of *diego*, or of any other of PCP gene, in the L/R organizer does not affect the directionality of genitalia rotation, suggesting that Diego does not play a critical role in *Drosophila* L/R asymmetry (supplementary material Table S1). In conclusion, the situs inversus proteins MyoID and Inversin, which play a central and upstream role in the establishment of L/R asymmetry, both require an interaction with the adherens junctions for their function.

It is important to note that the L/R axis is established after and, most importantly, relatively to the other two main axes, the anterior-posterior and dorsal-ventral axes (Hayashi and Murakami, 2001). Indeed, L/R determinants have to be oriented along existing spatial coordinates so that the L/R axis is positioned perpendicular to existing axes. We propose that the association of MyoID (and more generally of situs inversus proteins) with the adherens junctions is an essential mechanism to orient MyoID activity along the apical-basal axis, which in epithelia is perpendicular to the anterior-posterior axis and is thus equivalent to a dorsal-ventral axis. Therefore, association of MyoID with the adherens junctions would represent a way to orient and polarize its activity. Following polarization of MyoID in epithelia, the intrinsic chirality of myosins, through their directional activity towards one end of the actin filaments, could create de novo an asymmetric axis similar to the F-molecule model proposed by Brown and Wolpert (Brown and Wolpert, 1990).

In conclusion, our findings reveal an important link between the adherens junction and L/R asymmetry determinant in *Drosophila* and suggest an evolutionary conservation in vertebrates and invertebrates of the interactions between the adherens junction and the situs inversus proteins linking cell architecture and polarity to the patterning of the L/R axis. Future work on the molecular targets of MyoID and Inversin will help understand how the L/R axis becomes oriented to lead to stereotyped asymmetric organogenesis.

Acknowledgements

We are grateful to the anonymous reviewers for their constructive comments on the paper. We thank M. Mlodzik and E. Sanchez-Herrero for fly strains; and M. Clark and V. Van De Bor for critical reading of the manuscript. We thank the PRISM platform for its imaging facilities.

Funding

A.G.P. was funded by the Marie Curie Early Stage Training International PhD Program in Developmental and Cellular Decisions (InterDeC program) and the Association pour le Recherche contre le Cancer (ARC); P.S. by ARC; J.-B.C. is supported by the Agence Nationale de la Recherche (ANR) and Fondation pour

la Recherche Médicale (FRM). C.G. is supported by FRM and Institut National de la Santé et de la Recherche Médicale (INSERM). Work in the S.N. laboratory is supported by Centre National de la Recherche Scientifique (CNRS), ANR, ARC, European Molecular Biology Organization's Young Investigator Programme and FRM.

Competing interests statement

The authors declare no competing financial interests.

Supplementary material

Supplementary material available online at
http://dev.biologists.org/lookup/suppl/doi:10.1242/dev.047589/-/DC1

References

Ádám, G., Perrimon, N. and Noselli, S. (2003). The retinoic-like juvenile hormone controls the looping of left-right asymmetric organs in Drosophila. *Development* **130**, 2397-2406.

Aylsworth, A. S. (2001). Clinical aspects of defects in the determination of laterality. *Am. J. Med. Genet.* **101**, 345-355.

Brand, A. H. and Perrimon, N. (1993). Targeted gene expression as a means of altering cell fates and generating dominant phenotypes. *Development* **118**, 401-415.

Brown, N. A. and Wolpert, L. (1990). The development of handedness in left/right asymmetry. *Development* **109**, 1-9.

Coutelis, J. B., Petzoldt, A. G., Speder, P., Suzanne, M. and Noselli, S. (2008). Left-right asymmetry in Drosophila. *Semin. Cell Dev. Biol.* **19**, 252-262.

de Navas, L. F., Garaulet, D. L. and Sánchez-Herrero, E. (2006). The ultrabithorax Hox gene of Drosophila controls haltere size by regulating the Dpp pathway. *Development* **133**, 4495-4506.

Garcia-Castro, M. I., Vielmetter, E. and Bronner-Fraser, M. (2000). N-Cadherin, a cell adhesion molecule involved in establishment of embryonic left-right asymmetry. *Science* **288**, 1047-1051.

Hartenstein, V. (1993). *The Atlas of* Drosophila *Development*. Cold Spring Harbor, NY: Cold Spring Harbor Laboratory Press.

Hayashi, T. and Murakami, R. (2001). Left-right asymmetry in Drosophila melanogaster gut development. *Dev. Growth Differ.* **43**, 239-246.

Hegan, P. S., Mermall, V., Tilney, L. G. and Mooseker, M. S. (2007). Roles for Drosophila melanogaster myosin IB in maintenance of enterocyte brush-border structure and resistance to the bacterial pathogen Pseudomonas entomophila. *Mol. Biol. Cell* **18**, 4625-4636.

Hozumi, S., Maeda, R., Taniguchi, K., Kanai, M., Shirakabe, S., Sasamura, T., Speder, P., Noselli, S., Aigaki, T., Murakami, R. et al. (2006). An unconventional myosin in Drosophila reverses the default handedness in visceral organs. *Nature* **440**, 798-802.

Hozumi, S., Maeda, R., Taniguchi-Kanai, M., Okumura, T., Taniguchi, K., Kawakatsu, Y., Nakazawa, N., Hatori, R. and Matsuno, K. (2008). Head region of unconventional myosin I family members is responsible for the organ-specificity of their roles in left-right polarity in Drosophila. *Dev. Dyn.* **237**, 3528-3537.

Levin, M. (2006). Is the early left-right axis like a plant, a kidney, or a neuron? The integration of physiological signals in embryonic asymmetry. *Birth Defects Res. C. Embryo Today* **78**, 191-223.

Levin, M. and Palmer, A. R. (2007). Left-right patterning from the inside out: widespread evidence for intracellular control. *BioEssays* **29**, 271-287.

Levin, M., Thorlin, T., Robinson, K. R., Nogi, T. and Mercola, M. (2002). Asymmetries in H+/K+-ATPase and cell membrane potentials comprise a very early step in left-right patterning. *Cell* **111**, 77-89.

McGuire, S. E., Roman, G. and Davis, R. L. (2004). Gene expression systems in *Drosophila*: a synthesis of time and space. *Trends Genet.* **20**, 384-391.

Miyoshi, J. and Takai, Y. (2008). Structural and functional associations of apical junctions with cytoskeleton. *Biochim. Biophys. Acta* **1778**, 670-691.

Mooseker, M. S. and Cheney, R. E. (1995). Unconventional myosins. *Annu. Rev. Cell Dev. Biol.* **11**, 633-675.

Niessen, C. M. and Gottardi, C. J. (2008). Molecular components of the adherens junction. *Biochim. Biophys. Acta* **1778**, 562-571.

Nurnberger, J., Bacallao, R. L. and Phillips, C. L. (2002). Inversin forms a complex with catenins and N-cadherin in polarized epithelial cells. *Mol. Biol. Cell* **13**, 3096-3106.

Raya, A. and Belmonte, J. C. (2006). Left-right asymmetry in the vertebrate embryo: from early information to higher-level integration. *Nat. Rev. Genet.* **7**, 283-293.

Speder, P. and Noselli, S. (2007). Left-right asymmetry: class I myosins show the direction. *Curr. Opin. Cell Biol.* **19**, 82-87.

Speder, P., Adam, G. and Noselli, S. (2006). Type ID unconventional myosin controls left-right asymmetry in Drosophila. *Nature* **440**, 803-807.

Speder, P., Petzoldt, A., Suzanne, M. and Noselli, S. (2007). Strategies to establish left/right asymmetry in vertebrates and invertebrates. *Curr. Opin. Genet. Dev.* **17**, 351-358.

Suzanne, M., Petzoldt, A. G., Spéder, P., Coutelis, J. B., Stellers, H. and Noselli, S. (2010). Coupling of apoptosis and L/R patterning controls stepwise organ looping. *Curr. Biol.* **20**, 1773-1778.

Tabin, C. J. (2006). The key to left-right asymmetry. *Cell* **127**, 27-32.

Taniguchi, K., Maeda, R., Ando, T., Okumura, T., Nakazawa, N., Hatori, R., Nakamura, M., Hozumi, S., Fujiwara, H. and Matsuno, K. (2011). Chirality in planar cell shape contributes to left-right asymmetric epithelial morphogenesis. *Science* **333**, 339-341.

Yokoyama, T., Copeland, N. G., Jenkins, N. A., Montgomery, C. A., Elder, F. F. and Overbeek, P. A. (1993). Reversal of left-right asymmetry: a situs inversus mutation. *Science* **260**, 679-682.